RESULTS OF THE MODERNIZATION OF THE ELECTROSTATIC PRECIPITATOR AT UNIT B1 OF THE THERMAL POWER PLANT KOSTOLAC B

by

Milić D. ERIĆ[a*], Predrag LJ. STEFANOVIĆ[a], Zoran J. MARKOVIĆ[a], Rastko D. JOVANOVIĆ[a], Ivan M. LAZOVIĆ[a], Nikola V. ŽIVKOVIĆ[a], and Željko S. ILIĆ[b]

[a] University of Belgrade, Vinca Institute of Nuclear Sciences, Belgrade, Serbia
[b] Public Enterprise Electric Power Industry of Serbia, Thermal Power Plant Kostolac B, Kostolac, Serbia

Original scientific paper
https://doi.org/10.2298/TSCI18S5623E

The electrostatic precipitator system of the lignite fired 350 MWe unit B1 of Thermal Power Plant Kostolac B has been modernized during 2014. The results of complex in site measurements, performed in the frame of performance control test at the beginning of the exploitation period of the upgraded electrostatic precipitator proved that, under normal and guarantee working conditions of the boiler and precipitator, the emission of particulate matter do not exceed limiting value. After the period of precipitator further adjustments, five series of measurements in the frame of acceptance test were performed in accordance with relevant standards. This paper presents results of the investigation of particulate matter concentration, laboratory analysis of the lignite, fly and bottom ash samples, working parameters of the unit and upgraded electrostatic precipitator as well as results of the calculations. The averaged mean particulate concentration at the exit of upgraded electrostatic precipitator of the unit B1 during Acceptance test was below guaranteed value. It is confirmed that adjustments of electrostatic precipitator electrical parameters have improved electrostatic precipitator efficiency, as well that electrostatic precipitatorcould work highly efficiently in energy save mode with lower power consumption.

Key words: *emission, electrostatic precipitator, particulate matter, modernization*

Introduction

The success of an air pollution abatement program of any industrial facility ultimately depends upon effective design, operation and maintenance of installed air pollution control equipment, from which is required reliability, on-line availability, continuing regulatory compliance, and regulatory agency/source relations [1]. In the case of boilers fired with pulverized lignite, a dry electrostatic precipitation method is extensively used over large gas volumes, with a wide range of inlet temperatures, pressures, dust and acid gas conditions, requiring an electrostatic precipitator (ESP) efficiency of greater than 99.9%. The process performance mainly depends on the particle size distribution [2, 3], flow rate, particulate density and inlet

* Corresponding author, e-mail: milic@vinca.rs

concentration [4], particulate and flue gas resistance (influenced by the chemical composition of the ash) [5] and process temperature. Particles in the diameter range less than 1 μm are the most difficult to collect [6] because in this size range the fundamental field charging mechanism gives way to diffusion charging by thermal ions (random collisions). The preferred range of the resistivity is 10^8 to 10^{10} Ω cm [3], which is influenced by the chemical composition of the gas stream and particulate, the moisture and SO_x content of the gas stream and the temperature. A decrease in the sulfur content of lignite will generally result in an increase in resistivity and a reduction in the collection efficiency, while adequate amounts of *e. g.,* sodium and iron oxide can reduce resistivity and improve performance. One frequently used variation on the Deutsch-Anderson equation [7] for estimation of ESP collection efficiency, η_c [–], is the Matts-Ohnfeldt [8] version:

$$\eta_c = 1 - e^{-\left(\frac{Aw_k}{Q}\right)^k} \tag{1}$$

where A [m^2] is the total collection electrode surface area, Q [m^3s^{-1}] – the flue gas-flow rate, and w_k [m^2s^{-1}] is a modified migration (drift) velocity of particles (*i. e.*, it represents how quickly the charged gas particles move to the grounded collection electrode). Dimensionless parameter, k, depends on the process being evaluated, assumed to be independent of charging voltage and current levels, while particle chemical composition and size distribution within an ESP are assumed to be uniform as the gas stream moves through it. More generalized form of Deutsch based model for calculation of the overall collection efficiency, η_{TD}, determined as the sum of fractional collection efficiencies in all size intervals for a given particle size distribution, is described [6]:

$$\eta_{TD} = \sum_{d_{p\min}}^{d_{p\max}} \Delta R_{iz}(d_p)\,\eta_D(d_p) \tag{2}$$

where $\Delta R_{iz}(d_p)$ is percentage of dust particles of diameter, d_p, and:

$$\eta_D(d_p) = 1 - e^{-w(d_p)\frac{l}{bu}} = 1 - e^{-w(d_p)\frac{A}{Q}} \tag{3}$$

where $w(d_p)$ is migration velocity of a particle of diameter d_p [μm], b – the distance between the electrodes, u – the axial velocity of the flue gas, $A = 2hl$ – the area of two adjacent collecting electrodes, and $Q = 2hbu$ – the volume flow rate of the gas, l and h are the length and height of the collection electrode. Efficiency of precipitator could be increased by reducing spacing between plates, increasing precipitator length, reducing gas velocity, u, or increasing the drift velocity, w [9]. The designer must estimate or measure (if possible) the particle migration velocity, w, which could be expressed as [10]:

$$w(d_p) = \frac{d_p E_o E_p}{4\pi\mu} \tag{4}$$

where E_o [Vm^{-1}] is the strength of the field in which particles are charged, E_p [Vm^{-1}] – the strength of the field in which particles are collected, and μ [Pa·s] – the gas viscosity. Particle migration velocity depends on the voltage strength of both the charging and collection fields.

In order to increase drift velocity (and ESP efficiency) one must increase the average field strength, E_p, which is a function of both the applied electric voltage and the space charge current, and to improve plate rapping and gas distribution processes. Efforts to increase field strength have been realized by changing the geometry of the electrodes [11] so as to increase the current, by maintaining the operating voltage to near critical sparking levels by self-regulating power supplies as well as by increasing the distance between the electrodes *b*, and by field electrical sectionalization.

Equations (1) and (3) suggest that decrease in flue gas-flow results in an increase in collection efficiency and vice versa. When designing a new or reconstructing existing ESP, engineers typically base on a hypothetical average value for the gas velocity *u* through ESP, ignoring the localized velocity variations within the precipitator, with the primary aim of minimizing the loss potential through impact and re-inclusion [3]. This critical velocity is a function of flue gas-flow, plate shape and configuration [12], precipitator size and flue gas and particle resistivity.

Apart of the proper average value of *u* for the gas velocity through ESP, the gas-flow distribution in the ESP cross-sections should be uniform throughout the ESP (top to bottom, side to side). Therefore, the use of gas distribution devices such as perforated plates and turning vanes and good ductwork design (outlet as well as inlet one) are necessary in order to provide good gas distribution. Measurements [13] showed that the collection efficiency of ESP is rather complicated and highly related to inner gas-flow pattern. The dimensionless Bussinesk coefficient gives the measure of the achieved velocity field homogeneity in a transversal cross-section:

$$M_k = \frac{1}{S_k}\int\left(\frac{u}{u_k}\right)^2 \mathrm{d}S_k = \frac{1}{S_k}\sum_{i=1}^{n}\left(\frac{u_i}{u_k}\right)^2 \Delta S_{ki} \tag{5}$$

where u_i [m^2s^{-1}] is the mean velocity through the elementary surface *i* of the cross-section of the ESP chamber, u_k [m^2s^{-1}] – the mean velocity calculated for the whole cross-section of the ESP, S_k – the total area of the entire cross-section of the ESP chamber, ΔS_{ki} – the elementary surface *i*, in the cross-section of the ESP chamber, and *n* – the number of elementary surfaces *i* in the cross-section of the ESP chamber. According to the literature data, the Bussinesk coefficient should be ≤ 1.2 for highly efficient ESP.

Although the application of modern numerical simulation methods is increasingly more frequent with the development of computing technologies, numerical simulation of the fully coupled three coexisting fields of flue gas-flow, ash particle dynamics and electrostatics in the ESP chamber is still very demanding task and how a highly detailed geometry of the model is important for a strong simulation and reliable results [14]. Fulfilling mentioned demands simultaneously calls for an increase of active surface of the electrodes and improvement of flue gas distribution, which increase the volume and the weight of the ESP, or even ask for application of high frequency high voltage (HF HV) power supply [15] instead of transformer and the diode rectifier (T/R) set. The requirements [1] relating to particulate matter emission from large combustion plants have been incorporated into relevant Serbian legislation [16, 17]. The action plan for reconstruction and modernization of ESP systems of all thermal units within the Public Enterprise Electric Power Industry of Serbia (EPS) have been initiated since 2005 [18, 19]. The primary goal was to reduce annual emissions of particulate matter in the air from 66900 tons per year to the level of 5850 tons per year, giving the priority to the units under rehabilitation. Even more, environmental protection measures are needed

and the regulations covering the emission of dust from large power plants are being strengthened [20].

Modernization and optimization of ESP of TEKO B1 power unit was a complex task assisted by the results of measurements of the flue gas-flow field, temperature, composition and particle concentration at the entrance of and exit of the ESP, as well results of laboratory analysis of the lignite, fly and bottom ash taken during the measurements before and after modernization [21].

This paper presents results of the measurements and determination of particulate matter concentration, K_e, during the acceptance test. The results of the measurements confirmed that particulate matter concentration at the exit of the reconstructed ESP is below guaranteed values, thus proving the effectiveness of the ESP reconstruction and modernization undertaken.

Basic data of the upgraded unit TEKO B1

Unit B1 is operated as based load (continuous power generation ~6500 hours per year) with nominal power level of 348.5 MWe, steam production of 1000 ton per hour and boiler energy efficiency 87.8%. The TPP Kostolac B is burning lignite supplied from local open pit mine Drmno with a wide range of lignite characteristics. Prior to modernization of ESP of the TEKO B1 unit, the output particle concentration in flue gas were between 363 mg/m^3 and 603 mg/m^3 [16]. Even in the case of dedusting efficiency design value, the output particle concentration in flue gas still exceeded the new permissible value of 50 mg/Nm^3. The reconstruction of the boiler and turbine of the unit B1 was carried out during the 2014, fulfilling the goals of lowering emission of particulate matter and NO_x at continuous power level up to 350 MW. Simultaneously, the modernization of ESP of the TEKO B1 unit was done.

During the reconstruction the length of ESP was increased from 21.2 m to 29.2 m, the height of the ESP chamber is extended from 15.7 m to 21.0 m, while the width is increased from 2 m × 15.9 m to 21.2 m × 22.5 m (active width of electric fields 18.4 m × 18.4 m, active length of electric fields: 4.54 + 4.54 + 4.54 + 4.54 + 5.44 + 3.63 m). New bigger volume of ESP enabled an increase of the length and particulate residence time. The effective field height is extended to 15000 mm while spacing between the electrodes remains 300 mm (in zone 1) and 400 mm (in zones 2-6). A completely new flue gas ducts with shut-off dumpers (of the louvers type) and expansion joints as well new inlet hoods and outlet hoods were installed. Due to air preheater and flue gas fan foundation position, the inlet and outlet of the both ESP are not on the longitudinal axis of symmetry, fig. 1. Therefore flue gas ducts and hoods are equipped with new gas distribution blades to obtain uniform flue gas distribution profile and to decrease the erosive effect of the dust particles. Together with an increase in the cross-section of the ESP this resulted in a decrease of axial flue gas velocity through the ESP from 1.81 m/s to 1.372 m/s and in increase of flue gas and particles residence time from 9.6 seconds to 19 seconds.

New, bigger ESP housing enabled increase of collecting electrodes total area more than 2 times (from 2 m^2 × 19600 m^2, up to 88806 m^2). In order to reduce back corona and to increase efficiency, two discharge electrodes (of the needle type wire in the first four and wave type wire in the last two fields) are implemented per one collecting electrode (of the BE type). Upgraded ESP has 24 independent electrical fields, fig. 1, in four parallel series (two in the left ESP chamber and two in the right ESP chamber). Both left/right chamber of the ESP have 12 HV T/R units, in total 24 for the whole ESP.

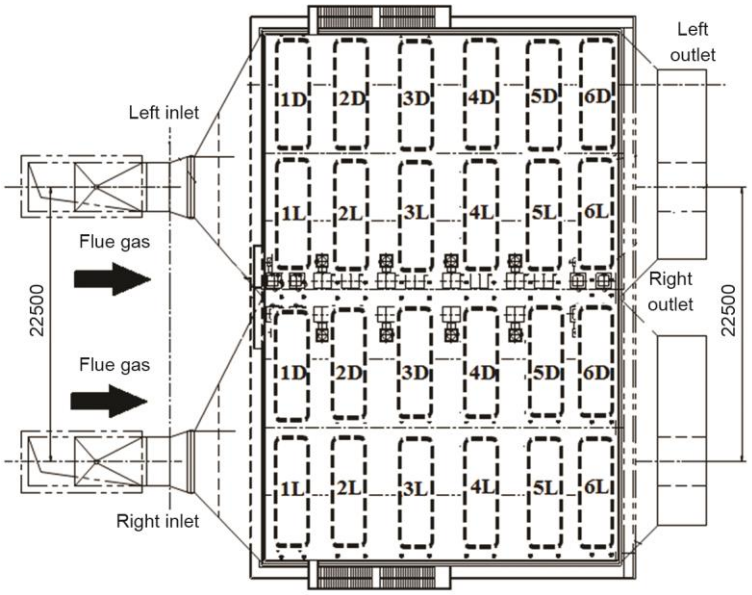

Figure 1. Location of the electrical fields in upgraded TEKO B1 ESP, horizontal cross-section

The electrical fields schematically presented in fig. 1 are numerated regarding the position in the ESP starting from inlet and the letter indicates left (L) or right (R) position in the ESP. A review of basic technical characteristics of the ESP before and after reconstruction is presented in tab. 1.

Table 1. Basic characteristic of the ESP of unit TEKO B1 before and after reconstruction

Characteristic	Unit	Before reconstruction	After reconstruction
Flow rate of flue gas, wet	Nm^3h^{-1}	1800000	1800870
Flue gas temperature	°C	150-200	180
Inlet dust concentration	gNm^{-3}	50.3 (wet gas)	67.1 max 75.6 (dry gas)
Precipitation efficiency	%	≥ 99.7	≥ 99.93
Outlet dust concentration	mg/Nm^{-3}	150 (wet gas)	≤ 50 (dry gas)
Electric zones along ESP	–	4	6
Max continuous voltage at the electrode	kV	–	72 (electric fields 1 and 6)
			66 (electric fields 2-5)
Max continuous current at the electrode	mA	–	1400 (electric field 1)
			1600 (electric fields 2-5)
			1000 (electric field 6)
Max continuous power per electric field	kVA		100.8 (electric fields 1) 105.6 (electric fields 2-5) 72 (electric field 6)

Overview of the results of performance test measurements series

Results of three measurements performed in the frame of the performance tests [21] indicated that measured outlet dust concentration, K_e^{outlet}, on the left ESP was lower (42.8, 42.2, and 40.7 mg/Nm^3) comparing to right ESP (49.0, 58.7, and 55.3 mg/Nm^3), still resulting in averaged mean particulate concentration of 48.11 mg/Nm^3 at the exit of upgraded ESP, *i. e.* below guaranteed value of 50 mg/Nm^3. The flue gas-flow rate and temperature were very stable but below guarantee values which was positive for ESP efficiency performance. Higher LHV value, lower moisture and ash content (compared to lignite guarantee values) also were in favor of the ESP high efficiency, except lower than guaranteed sulphure content. The collection (dedusting) efficiency, η, of the left part of ESP was close to guarantee value (99.92%), while efficiency of the right part of ESP was below guarantee value (99.86-99.89%) [21]. The collecting efficiency, η, was calculated:

$$\eta = 100\frac{K_e^{\text{inlet}} - (1+\Delta\alpha)K_e^{\text{outlet}}}{K_e^{\text{inlet}}} \tag{6}$$

where K_e^{inlet} is a dust concentration in flue gas before ESP, K_e^{outlet} – a dust concentration in flue gas at ESP exit, and $\Delta\alpha$ – the air leakage rate along left/right part of ESP determined by measurements and calculation of flue gas-flow rate at the left/right part of ESP inlet and exit. The total flue gas-flow through inlet of the ESP was around 10% lower than total flow through the outlet of the ESP. Subsequent inspection of the ESP found that some of the technical openings were not closed during the tests, which results in lower dedusting efficiency of the right ESP. Rapping system at the all four fields N^o 6 was turned off in the test N^o 1 and N^o 2 and was turned on before test N^o 3. Since the last fields separate the smallest particles and due to much longer rapping period (80-600 minutes) compared to test N^o 3 period (60 minutes), it had no significant effect on measured particulate matter concentration.

Results of the measurements and calculations in the frame of acceptance test

After the adjustments and optimization of the upgraded ESP, the series of five measurements were performed in the frame of acceptance test. The unit TEKO B1 was normaly operated with five mills, but at reduced parameters of live steam and unit power level (~336 MWe). Upgraded ESP of unit TEKO B1 was normaly operated, with maximum electric parameters at all electric fields during test N^o 1, 3, 4, and 5, while during test N^o 2 the ESP was working in the energy save mode, with lower power consumption of the ESP compared to other tests. Measuring cross-section at the inlet of the ESP is in horizontal flue gas channel (5 m wide with 4 measuring axes and 5.5 m deep with 4 measuring points) in front of left/right ESP chamber. Measuring cross-section at the exit of the ESP is positioned in vertical flue gas channel (4 m wide with 5 measuring axes and 4 m deep with 4-5 measuring points/axis) in front of left/right flue gas fan. The particulate matter measurements were performed with two in stack isokinetic sampling systems in accordance with ISO 9096:2003 and EN 13284-1.

Basic characteristics of lignite burned during Acceptance test are presented in tab. 2. The moisture content of lignite burned during first two tests was below design range while combustible content and LHV were higher than design values, which was in favor of high performance of the ESP. During tests N^o 3, 4, and 5, the LHV, combustibles and sulfur content of the lignite used were in the design range. The ash content and flue gas-flow rate were

Table 2. Basic lignite characteristics during acceptance test

Lignite quality	Unit	Guaranteed value	Measured value test 1	Measured value test 2	Measured value test 3	Measured value test 4	Measured value test 5
Lower heating value	$kJkg^{-1}$	6589	8735	9008	7750	7776	7865
Ash content	%	23.7	22.35	20.57	25.64	24.76	26.44
Combustible	%	32.00	38.52	40.17	35.11	35.74	35.36
Moisture content	%	44.4	39.13	39.26	39.25	39.49	38.20
Sulfur content	%	1.17	1.34	1.25	1.16	1.04	1.10
Carbon	%	20	25.38	25.93	22.63	22.85	23.13
Hydrogen	%	1.87	2.28	2.32	2.08	2.11	2.14
Sulfur – combustible	%		0.51	0.49	0.44	0.33	0.70
Nitrogen	%	8.96	0.41	0.40	0.37	0.39	0.38
Oxygen	%		9.94	11.04	9.58	10.06	9.01

higher than design values, resulting in very difficult conditions for high performance of the ESP. The unit operating parameters during the tests as well as results of particulate matter measurement for both ESP are presented in tab. 3. The flue gas temperature were very stable but below guarantee values which had positive impact on ESP efficiency performance. Particulate matter concentration at the exit of upgraded ESP of unit TEKO B1 was in the range 37.7-40.5 mg/Nm^3, *i. e.* below guaranteed value of 50 mg/Nm^3. Electrostatic precipitator efficiency, η, for both, left and right ESP, were equal or higher than guaranty value in tests N^o 1, 3, 4, and 5. A slightly lower than guaranty value (99.92%) of the ESP efficiency was obtained during the test N^o 2, when ESP was working in the energy save mode.

During the test N^o 1, 3, 4, and 5, upgraded ESP of unit B1 was normally operated, with stable voltage $U \approx 40$ kV and maximum specified value of current $I \approx 1400$ mA at electric fields in zone 1. In zones 2-5 measured current was at maximum specified value $I \approx 1600$ mA, while voltage was stable in the range 48-54 kV in zones 2-4 (depending on field) and 57-58 kV in zone 5. In zone 6 measured current was at maximum specified value $I \approx 1000$ mA, while voltage was very stable in the range 61-63 kV. During test 2 a stable maintenance of the set of ESP electrical parameters was also achieved, as can be seen from fig. 2 which represent the records during the test N^o 2 for the electrical fields 1D of the left (left diagram) and right (right diagram) ESP. During this test current was $I \approx 1150$ mA, less than maximum specified value.

The mean power consumption of whole ESP (taking into account both left and right chamber) during the tests N^o 1, 3, 4, and 5 were 2.235 MW. The mean power consumption during the test N^o 2, when ESP was operating in the energy save mode, was only 0.668 MW, retaining the dedusting efficiency at a satisfactory high level of 99.92%, very close to guarantee value. This indicates that most of the exploitation period ESP could work highly efficently in energy save mode with much lower power consumption.

Values of effective drift velocity, w_e, determined experimentally from commercial installations by using Deutch drift velocity [7] or modified drift velocity, w_k, given by eq. (1),

Table 3. The results of acceptance test of unit B1 upgraded ESP

Parameter		Unit	Guaranteed value	Measured value (L/R ESP)				
				Test 1	Test 2	Test 3	Test 4	Test 5
Gross unit power level		MW	350	336.18	334.67	336.02	336.19	336.06
Inlet flue gas temperature		°C	180	160.6/165.6	161.9/165.8	163.6/166.9	164.3/167.2	164.4/166.6
Flue gas-flow at operating conditions	left	m^3h^{-1}		1491961	1475027	1514175	1522119	1534472
	right			1534855	1549367	1608190	1621645	1633946
Wet flue gas-flow rate[1], inlet		Nm^3h^{-1}	1 800 870	1 817 434	1 808 982	1 864 281	1 869 289	1 879 314
Dust concentration at ESP exit [2]		$mgNm^{-3}$	< 50	38.47/39.59	38.74/40.06	39.76/40.54	37.66/38.71	38.72/39.83
Dust concentration at ESP inlet		gNm^{-1}	< 67.1	56.54	50.04	71.87	69.43	72.41
Dedusting efficiency, η[3]		%	99.93	99.93/99.93	99.92/99.92	99.94/99.94	99.94/99.94	99.95/99.94
ESP power consumption		kW		2232.6	668.2	2235.4	2235.4	2235.2

[1] at flue gas standard conditions: 0 °C, 101325 Pa, wet, O_2 = 6%,
[2] at flue gas conditions: 0 °C, 101325 Pa, dry, O_2 = 6%,
[3] calcualted according to eq. (6).

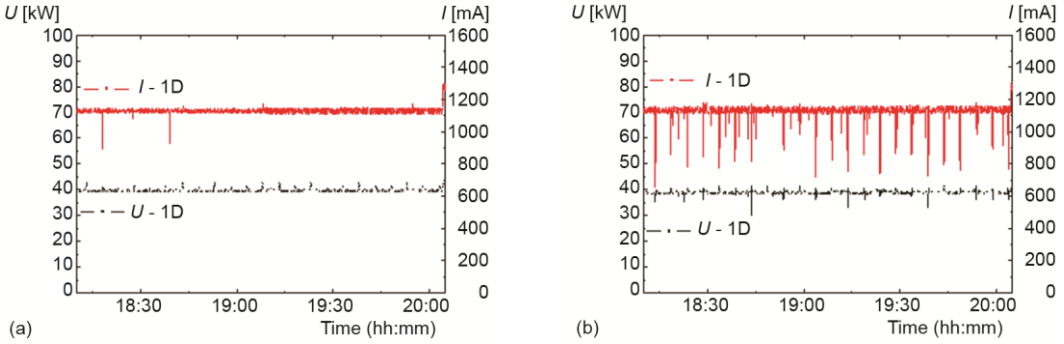

Figure 2. Working parameters of the electrical fields 1D of the left (left diagram) and right (right diagram) ESP during Acceptance test No 2 (unit B1 Control room data); (a) acceptance test #2, left ESP, zone I, section right, (b) acceptance test #2, right ESP, zone I, section right

do not agree with theoretical values obtained by using eq. (4) or other theoretical equations [10, 22]. In the theoretical calculation the effects of re-entrainment, which occurs during rapping or when there is uneven gas and dust distribution, have not been considered. One approach to overcome this situation is to determine modified migration velocity w_k by using the parameter k in the eq. (1) to simulate the increased difficulty to collect remaining dust as the precipitator becomes larger to reach very high collection efficiencies. For fly ash precipitation after lignite-fired boilers the value of k = 0.5 has turned out to be a reasonably good approximation for a variety of fuel and process condition [10].

Likewise, we can use the formal approach similar to eq. (1) in the reverse order, bypassing complex physical processes occurring in the ESP to certain extent, in order to determine the value of the effective drift velocity w_e [23]:

$$w_e = \frac{Q}{A}[-\ln(1-\eta)] \tag{7}$$

where η is calculated according to eq. (6). The precipitator efficiency as a function of effective drift velocity, w_e, for both left and right ESP chamber of the unit TEKO B1 is presented in fig. 3(b).

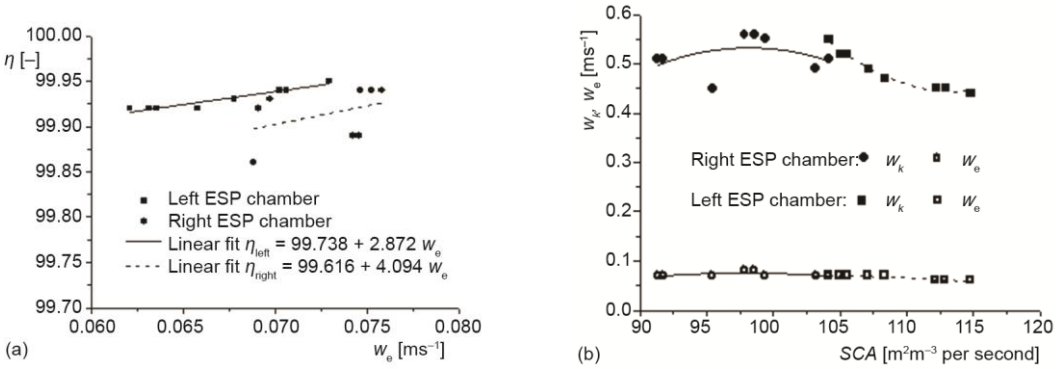

Figure 3. Unit TEKO B1 precipitator efficiency η as a function of effective drift velocity w_e (a) and modified w_k and effective we drift velocity *vs.* specific collection area (SCA) (b)

The effective drift velocity, w_e, takes into account all potential empirical influencing parameters such as the particle size distribution, the field strength, the gas composition, the space charge, *etc.* including special design features. For the same efficiency, η, the effective migration velocity of the right ESP chamber is higher than for the left one due the higher flue gas-flow. The further investigation of the relating electrical parameters of the matching electric fields is necessary in order to explain these differences. Supposing the same particle size distribution in the inlet of the chambers, the results for drift velocity, w_e, in addition of value of gas viscosity (related to gas composition and temperature), could be used by eq. (4) to check and adjust ESP electrical parameters of electrical fields.

Figure 3(b) specifies the migration velocity values obtained according to Deutch's, eq. (7), and Matts-Oehnfeldt, eq. (1) with $k = 0.5$, formulas for the left and right ESP chamber of unit TEKO B1, regarding the *SCA* value for each of chambers during the test. In general, higher migration velocities are obtained for the right ESP chamber. The migration velocities calculated by Deutch's formula show a gradual decrease with *SCA* for both ESP chambers. The smaller dispersion of almost constant values of w_e regarding flow rate is observed. The modified migration velocity w_k exhibit point of maximum for *SCA* value different for each chamber, giving the measurement relative to the efficiency per *SCA*.

The values of penetration $P = 100 - \eta$ [%] calculated according to results of series of measurements conducted in the frame of particulate emission guarantee tests of the upgraded ESP at unit A6 of TPP Nikola Tesla in city of Obrenovac, Serbia [18], as well as values of P calculated on the results of series of measurements conducted in the frame of particulate emission guarantee tests of the upgraded ESP at unit B2 of TPP KOSTOLAC-B [19] are presented

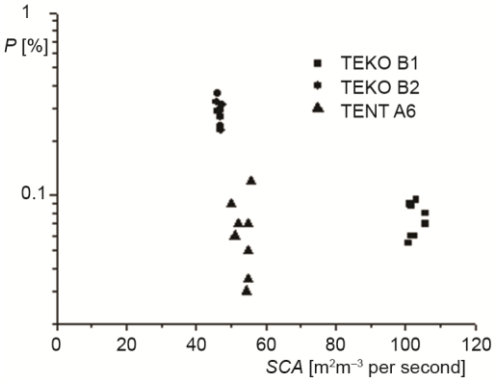

Figure 4. Penetration, *P*, as a function of specific collection area SCE for ESP of units TEKO B1, TEKO B2 and TENT A6

in fig. 4 along with values of *P* calculated for the TEKO B1 ESP. During these tests units achieved similar net power (334-336 MW for TEKO B1, 335-350 MW for TEKO B2 and 340-348 MW for TENT A6) and the ESP treated a similar quantity of the flue gas ($3.0\text{-}3.2\cdot10^6$ m^3/h for TEKO B1, $3.0\text{-}3.1\cdot10^6$ m^3/h for TEKO B2 and $2.8\text{-}3.1\cdot10^6$ m^3/h for TENT A6). The boilers of the units TEKO B1 and TEKO B2 are of the same design and they are burning the same Drmno lignite, but have a different ESP design. Among the other, the plate spacing in the TEKO B1 ESP is 300 mm in the first and 400 mm in the other five electrical fields, in regard to 400 mm in the first two and 500 mm in third and fourth electrical field of TEKO B2 ESP.

The unit TENT A6 is burning Kolubara lignite. The values of ash resistivity for this coal were similar to resistivity of ash of Drmno coal ($10^{12}\text{-}10^{13}$ Ω cm) and belong to the class of ashes of high resistivity, which have a negative impact on the ESP efficiency. The plate spacing of this ESP is 395 mm in all four electrical fields. A high dispersion of the *P* values for the unit TENT A6 was a consequence of significant changes of electrical parameters of the ESP [18] in order to determine optimum working regime. Nevertheless, one can see comparative advantage of TENT A6 ESP design over the other two, resulting in higher η for the similar *SCA* value comparing to the TEKO B2 ESP, and lower *SCA* values for similar η comparing to TEKO B1 ESP, thus proving decision to increase plate distance in this case of ash of higher resistivity.

Comparing values of *P* for TEKO B1 and TEKO B2, the larger plate spacing in case of TEKO B2 ESP results in significant decrease of *SCA*, but and lower η values also. For a case of higher ash resistivity, when plate spacing is increased from 300 mm to 400 mm some increase of η is found [24]. Since *SCA*, thus flue gas velocity, is restricted by ESP geometry, in addition to consideration of the differences in design and electrical working parameters of these ESPs, a further investigation of the flow field uniformity in transversal cross-sections of the TEKO B2 ESP chambers should be done, eq. 5, in order to find the cause of observed differences and to improve the TEKO B2 ESP efficiency.

Conclusion

By modernization of the unit TEKO B1 ESP a new bigger effective cross-section (2×276 m^2) and length/volume of ESP enabled high collecting surface (increased from 2×19600 m^2 to 88806 m^2), lower flue gas velocity (decreased from 1.81m/s to 1.372 m/s) and longer residence period in the electric field (increased from 9.6 seconds to 19 seconds). Both left/right chamber of the new ESP have 12 HV T/R units, in total 24 for whole ESP.

During the acceptance test, boiler of unit TEKO B1 was operated at reduced parameters of live steam and unit power level. Lignite used during first two tests was very good, with moisture content below design range, while combustible content and LHV were over design range, which was in favor of high performance of the ESP. The worse lignite was used during the tests N^o 3, 4, and 5 and flue gas-flow rate was higher than design value, resulting in

very difficult conditions for high performance of the ESP. The mean electric power consumption of the upgraded ESP during the test N^o 1, 3, 4, and 5 was 2.235 MW, while during test N^o 2 the ESP was working in the energy save mode, with much lesser power consumption. In all 5 tests, dust concentration of the particulate matter was in the range 37.7-40.5 mg/Nm^3, much lower than guarantee value (<50 mg/Nm^3) although the conditions for high performance of ESP were very difficult. During regimes 3, 4, and 5 the inlet dust concentration was near to maximum projected value and flue gas-flow rate was over design value. It could be concluded that ESP has capabilties to work highly efficient in more difficult conditions. Collection efficiency of the ESP in test N^o 1 was at guarantee value, while in test N^o 2 was near guarantee value (99.92%). The results in test N^o 2 when low exit dust concentration is obtained in energy save mode indicate that most of the working period, ESP could work highly efficently with low electric power consumption. Although very difficult conditions for ESP high efficiency performance in tests N^o 3, 4, and 5, collection efficiency of the ESP was higher than guarantee value. As a result of Acceptance test, the average mean particulate concentration at the exit of upgraded ESP was found to be 39.2 mg/Nm^3.

Acknowledgment

The authors would like to acknowledge their high appreciation to the Ministry of Education, Science and Technological Development of Republic of Serbia (Project No. III42010 *Reduction of Air Pollution from Thermal Power Plants of the PE Electric Power Industry of Serbia* and Project No. TR33050) and Public Enterprise *Electric Power Industry of Serbia*, Belgrade, Serbia for the support.

Nomenclature

A – collection electrode area, [m^2]
b – distance between the electrodes, [m]
d_p – diameter of particle, [m]
E_o, E_p – strength of the field, [Vm^{-1}]
l, h – length, height of the collection electrode, [m]
K_e^{inlet} – dust concentration in flue gas before ESP, [gNm^{-3}]
K_e^{outlet} – dust concentration in flue gas at ESP exit [mgNm^{-3}]
M_k – dimensionless Bussinesk coefficient, [–]
n – number of elementary surfaces i in the cross-section of the ESP, [–]
$\Delta R_{iz}(d_p)$ – percentage of dust particles in the i-th interval, [%]
ΔS_{ki} – elementary surface i, [m^2]
Q – flue gas-flow rate, [m^{3}s^{-1}]
u – axial velocity of the flue gas, [m^{2}s^{-1}]
w_e, w_k – effective and modified migration (drift) velocity of particles, [m^{2}s^{-1}]

Greek symbols

μ – gas viscosity, [Pa·s]
η, η_C, η_{TD} – collection efficiency, [–]

References

[1] ***, Directive 2001/80/EC of the European Parliament and of the Council of 23 October 2001 on the limitation of emissions of certain pollutants into the air from large combustion plants
[2] White, H. J., Electrostatic Precipitation of Fly Ash, *Journal of the Air Pollution Control Association*, *27* (1997), 1, pp. 15-22
[3] Reynolds, J. P., *et al.*, Calculating Collection Efficiencies for Electrostatic Precipitators, *Journal of the Air Pollution Control Association*, *25* (1975), 6, pp. 610-616
[4] Saunders, L.,G., *et al.*, Operation and Maintenance Manual for Electrostatic Precipitators, Report No. EPA/625/1-85/017, Air and Energy Engineering Research Laboratory, Office of Research and Development, U.S. Environmental Protection Agency, New York, USA, 1985
[5] White, H. J., Electrical Resistivity of Fly Ash, *Air Repair*, 3 (1953), 2, pp. 79-86
[6] Swierczok, A., Jedrusik, M., The Collection Efficiency of ESP Model – Comparison of Experimental Results and Calculations using Deutsch Model, *Journal of Electrostatics*, *91* (2018), Feb., pp. 41-47

[7] Deutsch, W., Bewegung und Ladung der Elektrizitatstrager im Zylinderkondensator, *Annalen der Physik*, *373* (1992), 12, pp. 335-344
[8] Matts, S., Ohnfeldt, P. O., Efficient Gas Cleaning with S. F. Electrostatic Precipitators, Flakt. A. B. Swenska FlaktFabriken, June, 1973
[9] Lagarias, J. S., Predicting Performance of Electrostatic Precipitators, *Journal of the Air Pollution Control Association*, *13*, (1963), 12, pp. 595-599
[10] Back, A., Some Observations Regarding the Matts-Öhnfeldt Equation, *Proceedings*, International Symposium ICESP XIII, Bangalore, India, 2013
[11] Nielsen, N. F., Andersson, C., Electrode Shape and Collector Plate Spacing Effects on ESP Performance, in: *Electrostatic Precipitation*, (Ed. Yan K.). Springer, Berlin, Heidelberg, Germany, 2009
[12] Ning, Z., *et al.*, Electrode Configurations Inside an Electrostatic Precipitator and their Impact on Collection Efficiency and Flow Pattern, *The European Physical Journal D*, *70* (2016), June, pp. 126-?
[13] Jedrusik, M., *et al.*, Physical and Numerical Modelling of Gas Flow in Electrostatic Precipitator, *Przegląd Elektrotechniczny*, *93* (2017), 2, pp. 228-231
[14] Shah, M. E., *et al.*, Influence of the Inlet Velocity Profiles on the Prediction of Velocity Distribution Inside an Electrostatic Precipitator, *Experimental Thermal and Fluid Science*, *33* (2009), 2, pp. 322-328
[15] Vukosavić, S., High Frequency Power Supply for Electrostatic Precipitators in Thermal Power Plants, *Electronics*, *15* (2011), 1, pp. 11-20
[16] Gavrić, M., *et al.*, Green Book of the Electric Power Industry of Serbia, (in Serbian), Belgrade, Serbia, 2009, www.eps.rs
[17] Oka, S., Strategy of Energy Sector Development in the Republic of Serbia until 2015, (in Serbian), *Termotehnika*, *31* (2005), 1-2, pp. 13-70
[18] Erić, M., *et al.*, Particulate Matter Emission Investigation on the Upgraded Elecrostatic Precipitators at TPP Nikola Tesla, *Proceedings*, 15th Symposium on Thermal Science and Engineering of Serbia, Soko Banja, Serbia, 2011, pp. 568-577
[19] Erić, M., *et al.*, Reduction of Particulate Matter Emission of the Upgraded Electrostatic Precipitators at Unit B2 of the TPP Nikola Tesla, *Proceedings*,16th Symposium on Thermal Science and Engineering of Serbia, Soko Banja, Serbia, 2013, pp. 750-757
[20] *** Interinstitutional File: 2013/0443 (COD), Council of the European Union, http://data.consilium.europa.eu/doc/document/ST-10607-2016-INIT/en/pdf
[21] Erić, M., Reduction of Particulate Matter Emission by the Modernization of the Electrostatic Precipitators at Unit B1 of the TPP Kostolac B, *Proceedings*, 17th Symposium on Thermal Science and Engineering of Serbia, Sokobanja, Serbia, 2015, pp. 569-576
[22] Kim, S. H., Lee, K. W., Experimental Study of Electrostatic Precipitator Performance and Comparison with Existing Theoretical Prediction Models, *Journal of Electrostatics*, *48* (1999), 1, pp. 3-25
[23] *** VDI 3678 Part 1 Electrostatic Precipitators – Process and Waste Gas Cleaning, Verein Deutcher Ingenieure e.V., Dusseldorf, 2011, (in English)
[24] Navarrete, B., *et al.*, Influence of Plate Spacing and Ash Resistivity on the Efficiency of Electrostatic Precipitators, *Journal of Electrostatics*, *39* (1997), pp. 65-81

Paper submitted: August 9, 2018
Paper revised: October 29 2018
Paper accepted: October 31, 2018